PERFORMANCE ANALYSIS OF DFIG WIND TURBINES WITH CROWBAR PROTECTION UNDER SHOR CIRCUIT

Patel Poonam J[1], Prof. Hardik Raval[2], Prof. A.M.Patel[3]
[1]PG scholar, [2,3]Assistant Professor
Electrical Department, MEC, [2]Basna, [3]Palanpur. Gujarat, India

Abstract: Doubly Fed Induction Generators DFIG are nowadays widely used in variable speed wind power plants. The dynamic interaction between variable speed DFIG wind turbines and the power system which is subjected to disturbances, such as short circuit faults, is an important issue. The ability of the wind power plant to stay connected to the grid during disturbances is important to avoid a cascading effect due to lack of power. This paper investigates the impact of fault ride through on the stability of DFIG wind turbine using crowbar resistance. Simulation test using MATLAB-Simulink toolbox is implemented on a 9 MW wind farm exports its power to 120 KV grid. The simulation is performed using different crowbar resistances. The variations of rotor current, rotor speed, DC-link voltage, active power and reactive power of the wind farm are investigated.

Index Terms- DFIG, Crowbar Resistance, Rotor Current, Active Power, Reactive Power, Short Circuit.

I. INTRODUCTION

Due to the increasing of CO 2 emissions, renewable energy systems, especially wind energy generation, have attracted great interest in recent years. Nowadays, the most widely used wind turbines in wind farm are based on DFIG due to some advantages such as reduction of inverter cost, the potential to control torque and a slight increase in efficiency of wind energy extraction. However, wind turbines based on the DFIG are very sensitive to grid disturbance especially to voltage dips [1]. DFIG power converter, which has a restricted over-current limit, needs special attention especially during faults in the grid. When faults occur and cause voltage dips, subsequently the current flowing through the power converter may be very high over-current. During this situation, it is common to block the converter to avoid any risk of damage, and then to disconnect the generator from the grid. The most demanding requisite for wind farms especially with DFIG is the Fault Ride Through FRT capability. The wind farm must stay connected to the grid during system disturbances and support the network voltage and frequency. This implies some requirements for the safe operation of the rotor side inverter of the DFIG, since the rotor current will become very large during these grid failures. Therefore, DFIG requires a protection system called active crowbar disconnects the converter in order to protect it turning the generator into a squirrel cage induction machine [2-3]. The crowbar may comprise of a set of thyristors that will short- circuit the rotor windings when triggered and thereby limit the rotor voltage and provide an additional path for the rotor current. Different values of the crowbar resistors result in a different behavior. Using this technology, the DFIG can stay connected to the grid and resume operation as soon as possible. Several research works have dealt with different crowbar strategies for Low Voltage Ride Through LVRT improvement [4-9]. The value of crowbar resistance should be chosen carefully. There are two requirements that give an upper and a lower limit to the crowbar resistance. It should be high enough to limit the short circuit rotor current and it should be low enough to avoid too high voltage in the rotor circuit. Motivated by the reason above, this paper provides a study of the dynamics of the grid connected with DFIG wind turbine. This paper investigates a model of 9 MW wind farm exports its power to a 120 KV grid. The simulation is investigated using SimPowerSystem toolbox. The impact of different crowbar resistance on the behavior of DFIG wind turbine during fault is investigated. The crowbar resistances are simulated as a symmetric three phase Y-connection.

II. DFIG MODEL

In order to model the DFIG, a standard wound-rotor induction machine component from the Sim Power System toolbox has been used. The synchronous d–q reference frame has been selected to perform all the simulations [10-11]:

$$v_{ds} = -R_s i_{ds} - \omega_s \psi_{qs} + \frac{d\psi_{ds}}{dt} \quad (1)$$

$$v_{qs} = -R_s i_{qs} - \omega_s \psi_{ds} + \frac{d\psi_{qs}}{dt} \quad (2)$$

$$v_{dr} = -R_r i_{dr} - \omega_r \psi_{qr} + \frac{d\psi_{dr}}{dt} \quad (3)$$

$$v_{qr} = -R_r i_{qr} - \omega_r \psi_{dr} + \frac{d\psi_{qr}}{dt} \quad (4)$$

where v are voltages (V), i are currents(A), R are resistances (Ω), ψ are flux linkages (V·s). Indices d and q indicate direct and quadrature axis components respectively while s and r indicate stator and rotor quantities respectively. All quantities are referred to the stator.

III. DFIG CONTROL

Figure 1 shows the schematic diagram of a DFIG connected to grid. It consists of a wound rotor induction generator with back-to-back voltage source converters linking the rotor to the grid. The back-to-back converter consists of a Rotor Side Converter (RSC) and a Grid Side Converter (GSC) connected to the grid by a line filter to reduce the harmonics

caused by the converter. The RSC is used to control the generator speed and reactive power, while the GSC is used to control DC-link voltage and reactive power exchange with the grid [12].

A. Rotor Side Converter Control System

The RSC controls independently the active and reactive power injected by the DFIG into the grid in a stator flux dqreference frame. Figure 2 shows the control scheme of the RSC. The q-axis current component Iqris used to control theactive power using a maximum power tracking strategy to calculate the active power reference [10]. The actual speed of the turbine ωris measured and the corresponding mechanical power of the tracking characteristic is used as the reference power for the power control loop. The reference value for the active power Pris compared with its actual value P and the error is sent to a PI controller which generates the reference value for the q-axis current Iqr_erf. This signal is compared to its actual value Iqrand the error is passed through a second PI controller determining the reference voltage for the q-axis componentVqr. The d-axis is used to control the reactive power exchanged with the grid, which in normal operation is set to zero in order to operate with unity power factor. In case of disturbance, if the induced current in the rotor circuit is not high enough to trigger the over-current protection, the RSC is set to inject reactive power into the grid in order to support the voltage restoration. In such case, the actual voltage V at the collection bus is compared to its reference value Vrefand the error is passed through a PI controller to generate the reference signal for the reactive power of the DFIG. Similar to the control strategy of the q component, the error between the reactive power reference and its actual value isss passed through a PI controller to determine the reference value for the d-axis current Idr_erf. This signal is compared to the d-axis current value Idrand the error is sent to a third PI controller which determines the reference voltage for the d-axis component Vdr.

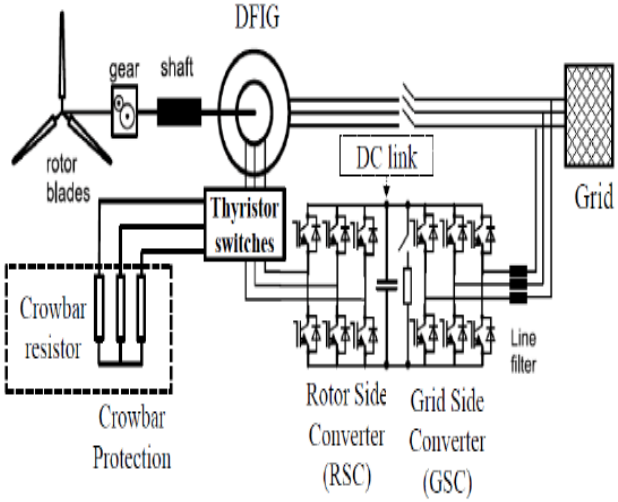

Figure 1 Doubly fed induction generator controller

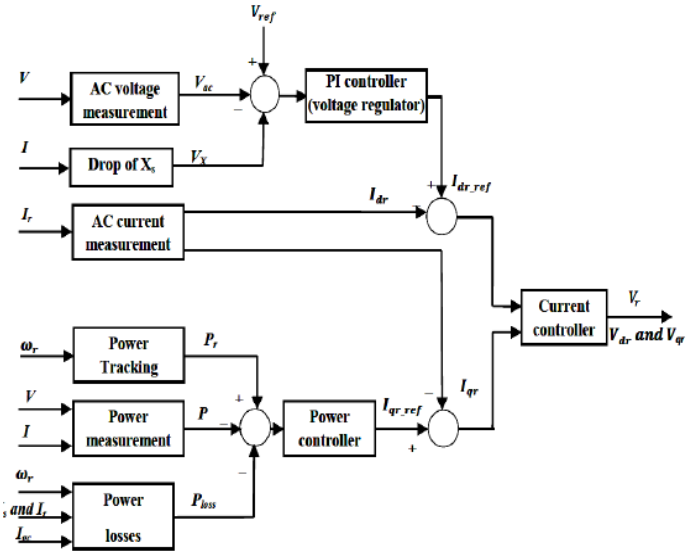

Figure 2 Schematic diagram of rotor side converter control system.

B. Grid Side Converter Control System

Figure 3 shows the control system of the GSC which is used to regulate the DC link voltage between both converters. In normal operation, the RSC already controls the unity power factor operation and therefore the reference value for the exchanged reactive power between the GSC and the grid is set to zero. In case of disturbance, the GSC is set to inject reactive power into the grid whether the RSC is blocked or is kept in operation. The control of the GSC is performed using the dqreference frame. The actual voltage Vdcat the DC link is compared with its reference value Vdc_refand the error between both signals is passed through a PI controller which determines the reference signal for the d-axis current Id_gsc_ref. This latter signal is subtracted with its current value Id_gscand the error is sent to another PI controller to obtain the reference voltage for the d-axis component. As for the q-axis current, its reference value depends whether the system operates in normal operation or during disturbance.

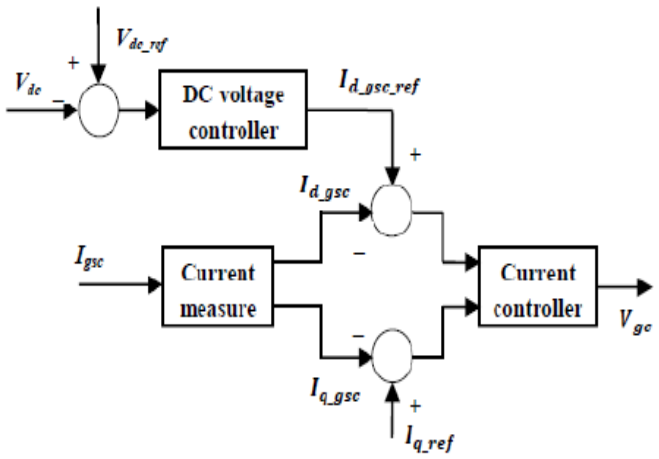

Figure 3 Schematic diagram of grid side converter control.

In case of disturbance, the actual AC-side voltage of the GSC is compared with its reference value and the error is passed through a PI controller which generates the reference signal for the q-axis current. This reference signal is compared to its current value and the error is sent to a second PI controller which establishes the reference voltage for the q axis component. The injection of active and reactive power by the GSC is limited by its nominal capacity represented by the following equation in per unit base:

$$|I_{conv}| = \sqrt{(I_q)^2 + (I_d)^2} \le 1 \qquad (5)$$

During normal operation, the strategy does not present limitations with the control of the DC link voltage since the qaxiscurrent is set to zero and therefore the converter capacity is only used to control the DC link voltage.

IV. DYNAMIC SIMULATION

To demonstrate the effect of a grid fault on a DFIG wind farm connected grid, a detailed time domain model is investigated.Figure 4 shows a single line diagram of the studied system. It consists of six 1.5 MW wind turbines connected to a 25-kV distribution system exports power to a 120-kV grid through a 30 km transmission line. The stator windings are connected directly to the 60 Hz grid while the rotor is fed at variable frequency through the RSC converter. The GSC is connected to the grid by a line filter to reduce the harmonics caused by the converter. The wind turbine has a protection system monitoring voltage, current and machine speed. The DC link voltage of the DFIG is also monitored. In this paper, the simulated disturbance is a three-phase to ground fault occurs at the wind farm terminals for 150 ms duration, where the protection system detects it after 10 ms from its occurrence. When the fault is detected by the protection system, the thyristors of the crowbar are switched on and the RSC is kept open. At the same time the rotor current is flowing through the crowbar resistor. When the crowbar is activated the RSC pulses are disabled and the machine behaves like a squirrel cage induction machine directly coupled to the grid. After fault clearance, the crowbar resistance is still connected for 10 ms and then the RSC is reconnected. The main data of DFIG wind farm and system parameters are illustrated in Appendix A. The simulation scenario is performed for different crowbar resistance values as shown in Table 1.

Table 1: Relations between crowbar resistance and rotor resistance

Case 1	without crowbar resistance
Case 2	crowbar resistance = 10 × rotor resistance
Case 3	crowbar resistance = 50 × rotor resistance
Case 4	crowbar resistance = 100 × rotor resistance

A simplified aerodynamic model is normally used when the electrical behavior of the wind turbine is the main interest of the study. The aerodynamic torque, which is ratio of rotor power and rotor speed, is given by equation,

$$T = \frac{Power}{\omega_r} = \frac{1}{2}\frac{\pi r_r{}^2 V_w{}^3 \rho C_p}{\omega_r}$$

Where, $Cp(\lambda,\beta)$ = Power co-efficient

$$Cp(\lambda,\beta) = 0.22(\frac{116}{\lambda i} - 0.4\lambda - 5.0)e\text{^}(\frac{-12.5}{\lambda i})$$

with,

$$\lambda i = \frac{1}{\frac{1}{\lambda + 0.08\beta} - \frac{0.035}{\beta\text{^}3+1}}$$

Figure 5 shows the wind turbine power characteristics at different wind speed values when the pitch angle is zero. For a wind speed of 10 m/s, the maximum turbine output is 0.55 puof its rated power.

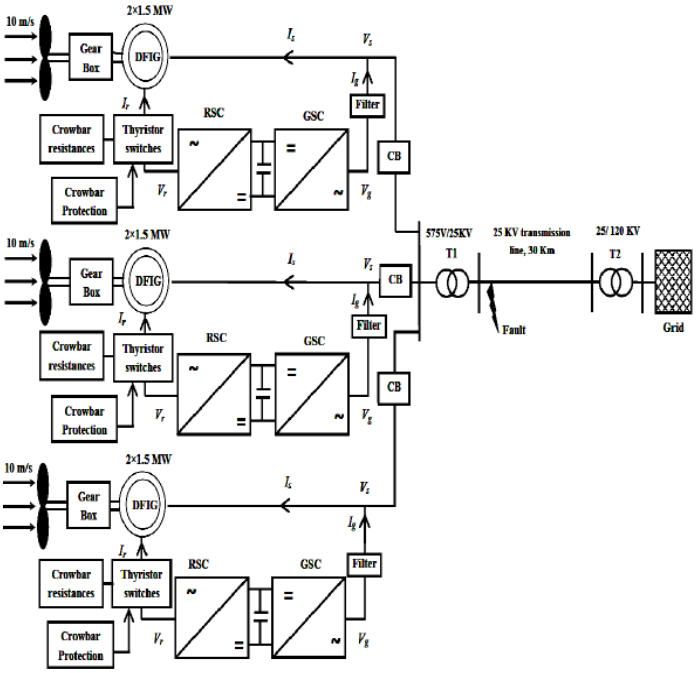

Figure 4 Single line diagram of the studied system

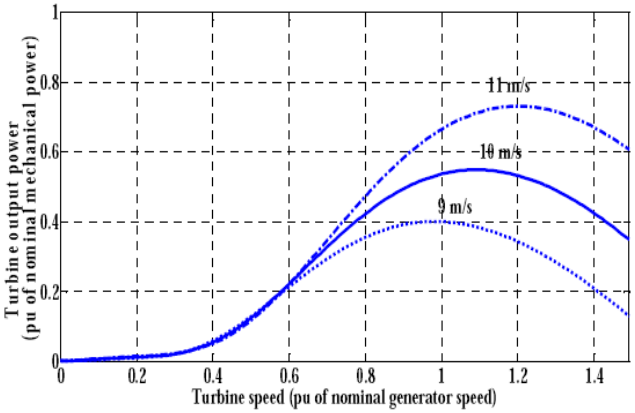

Figure 5 Turbine power characteristic with zero pitch angle.

V. SIMULATION RESULTS

The simulation results show the variations of rotor current, rotor speed, active power, reactive power, and DC link voltage with different crowbar resistors during grid faults. As shown in Fig. 6, the rotor current is decreased by increasing the crowbar resistance value. Also, the post fault current is affected by the crowbar resistance value. As shown in Fig. 6 (a), the post fault current is varied between 1.6 pu and 1.4 pu when the crowbar resistance is not used. In case of using the crowbar resistance equals to 10 times of rotor resistance, the post fault current is varied between 0.88 pu and 0.91 pu as shown in Fig. 6 (b). It is noticed that when the crowbar resistance is increased to 50 times or 100 times of rotor resistance, the post fault current has the same trend and varied between 0.73 pu and 0.85 pu.

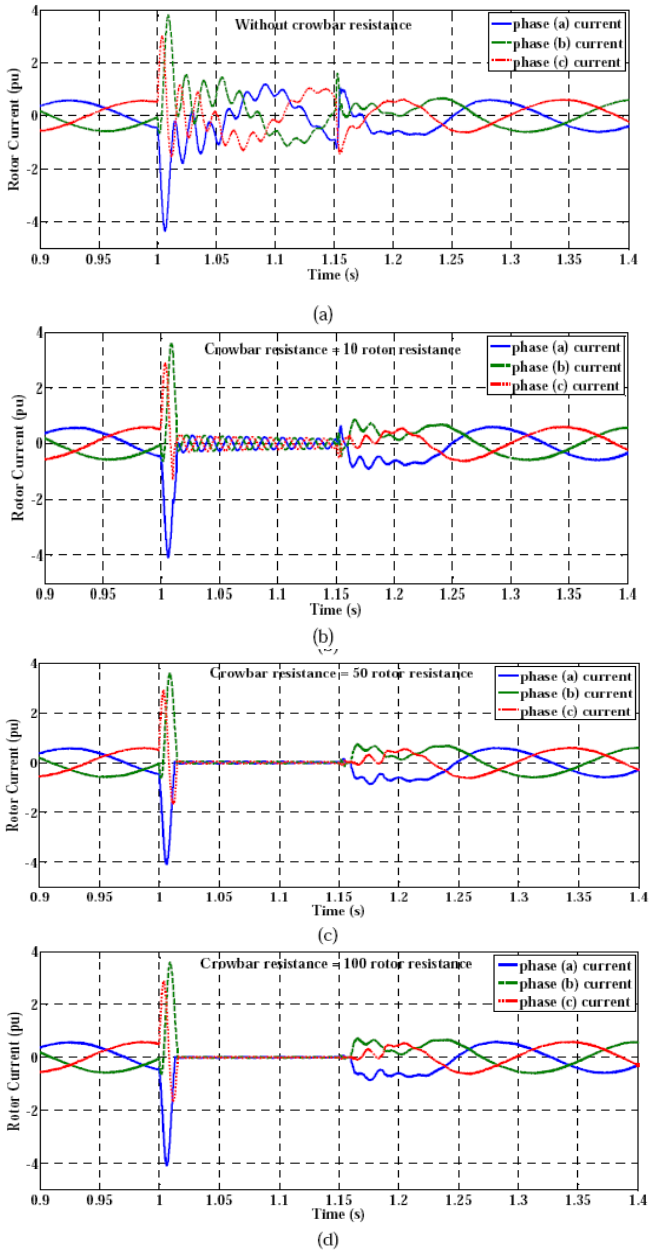

Figure 6 Rotor current versus time for different crowbar resistances

a) without crowbar resistance.
b) crowbar resistance = 10 times of rotor resistance.
c) crowbar resistance = 50 times of rotor resistance.
d) crowbar resistance = 100times of rotor resistance.

Figure 7 shows the variations of rotor speed during fault with different crowbar resistances. After fault occurrence and before the crowbar is activated, the rotor speed is decreased from 1.09 pu to 1.0891 pu. The rotor speed is increased rapidly after activating of crowbar resistance. It is noticed that the peak value of rotor resistance is increased by increasing the crowbar resistance value. The rotor speed is varied between 1.0955 pu and 1.097 pu according the crowbar resistance value.

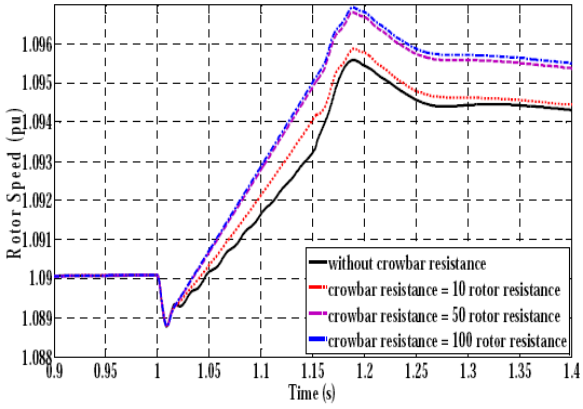

Figure 7 Rotor speed variations during fault with different crowbar resistances.

Figure 8 shows the variations of the generated active power during fault in case of different crowbar resistances. Before fault occurrence, the total generated active power is 4.7 MW where the wind farm operates at wind speed of 10 m/s. During fault, the generated active power is decreased to 1.68 MW when crowbar resistance is not used while it decreases to 0.47 MW when the crowbar resistance is activated for different values. After fault clearance and reconnection of the RSC converter, the generated active power is increased to 7 MW for all studied cases and then the system returns to the steady state operation. Figure 9 shows the variations of the reactive power during fault in case of different crowbar resistances. Before fault occurrence, the reactive power is nearly zero. After fault occurrence, in case of crowbar resistance is not activated, the RSC converter acts as STATCOM and injects 5.95 MVAR reactive power to the grid. During fault period, when there is no crowbar resistance, the reactive power is varied between 0.98 MVAR as absorbed reactive power and 0.4 MVAR as injected reactive power. In the case of crowbar resistance is activated, the wind farm generators absorb reactive power of 0.4 MVAR for different values of crowbar resistance. After fault clearance, the reactive power is exchanged between the wind farm and the grid before the system returns to the steady state operation. After fault clearance and reconnection of RSC, the injected reactive power is increased to 3.5 MVAR when the crowbar resistance equals 10 times of rotor

resistance. Also, it is increased to 3.95 MVAR when the crowbar resistance equals 50 and 100 times of rotor resistance, where it was 2.9 MVAR when the crowbar protection is not used. On the other hand, the absorbed reactive power is increased to 3.5 MVAR when there is no crowbar resistance and it equals 2.5 MVAR when the crowbar protection is used for all cases.

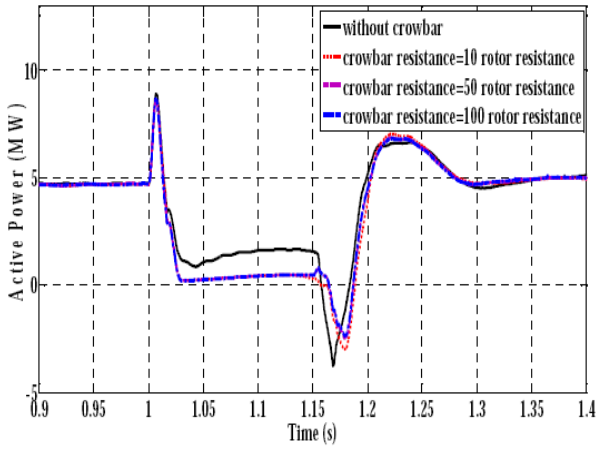

Figure 8 Active power variations of DFIG wind farm during fault with different crowbar resistances.

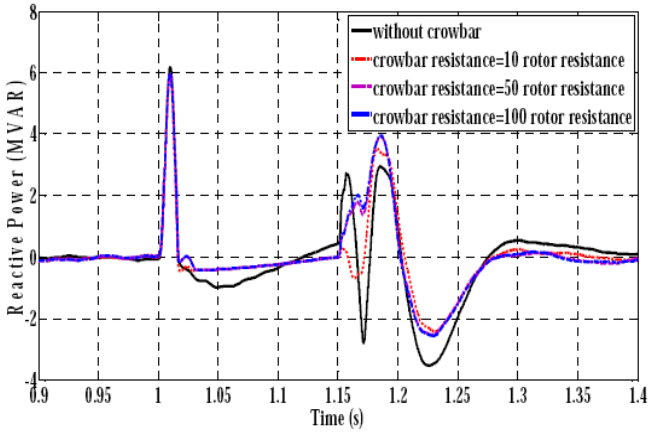

Figure 9 Reactive power variations of DFIG wind farm during fault with different crowbar resistances.

Figure 10 shows the variations of the DC-link voltage during fault with different crowbar resistances. The DC-link capacitance equals 60 mF with nominal voltage of 1200 V. During fault occurrence, the grid voltage falls and the GSC is not able to transfer the power from the RSC to the grid. Therefore, the additional energy goes into charging the DClink capacitor and thus its voltage rises rapidly. When the system operates without crowbar protection, the DC-link voltage is increased to 2090 V during fault period. When the crowbar resistance is triggered at the instant of 1.01 s, the DClink voltage value is 1716 V and starts to decrease for the case of crowbar resistance equals 10 times of rotor resistances. But for other two cases, it will continue in increasing until it reaches 1814 V and then starts in decreasing.

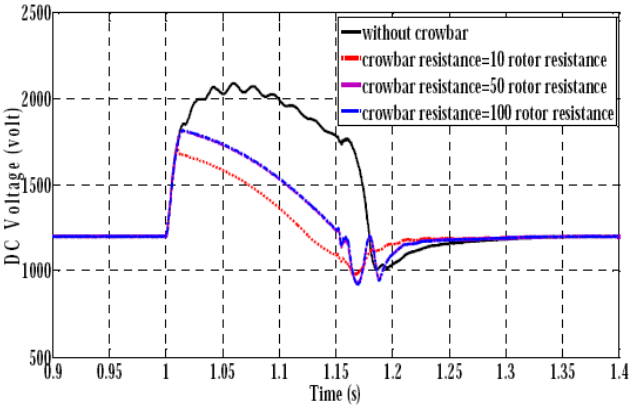

Figure 10 DC-link voltage variations during fault with different crowbar resistances.

VI. CONCLUSIONS

This paper investigates the behavior of DFIG wind farm during terminal fault in presence of crowbar protection system.. The simulation scenario is performed for different crowbar resistances values. The simulated disturbance is a three-phase to ground fault occurs at the wind farm terminals for 150 ms duration. The crowbar protection resistance is activated after fault occurrence with delay time of 10 ms. Also, it will deactivated after fault clearance with delay time of 10 ms. It shows that absence of crowbar resistance leads to high rotor current, high DC-link voltage and more reactive power fluctuations during and post fault periods. When the crowbar protection is used, rotor current is decreased while rotor speed is increased. When the crowbar protection is not used, the generated active power value during fault is more than that in the cases of using crowbar resistances. After fault clearance and reconnection of RSC, the DFIG can provide reactive power support to the grid and thus help in stabilizing of the grid voltage. Finally, the rotor current, rotor speed, DC-link voltage, active power and reactive power are affected by a certain value of the crowbar resistance. Therefore, the crowbar resistance value should be chosen carefully.

APPENDIX A. DFIG DATA AND SYSTEM PARAMETERS

DFIG parameters
Rated power (MW) 1.5
Rated voltage (V) 575
Rated frequency (Hz) 60
Stator resistance (pu) 0.004843
Rotor resistance (pu) 0.004377
Stator leakage inductance (pu) 0.1248
Rotor leakage inductance (pu) 0.1791
Mutual inductance (pu) 6.77
Transmission line parameters
Positive sequence resistance (ohm/km) 0.1153
Zero sequence resistance (ohm/km) 0.413
Positive sequence inductance (henries/km) 0.00105
Zero sequence inductance (henries/km) 0.00332
Positive sequence capacitance (farads/km) 11.33e-9

Zero sequence capacitance (farads/km) 5.01e-9
Transformer(T1) parameter
Rated power (MVA) 12
Turns ratio 575V/25KV
Impedance (pu) 0.0017+j0.05
Transformer(T2) parameter
Rated power (MVA) 47
Turns ratio 25KV/120KV
Impedance (pu) 0.00534+j0.16
Grid impedance
Impedance (pu) 0.0004+j0.004

REFERENCES

[1] Min Min Kyaw, V.K. Ramachandaramurthy, "Fault ride through and voltage regulation for grid connected wind turbine", Science Direct, Renewable Energy 36 (2011) 206-215, doi:10.1016/j.renene.2010.06.022.
[2] L. Shi, N. Chen and Q. Lu, "Dynamic Characteristic Analysis of Doublyfed Induction Generator Low Voltage Ride-through", ScienceDirect, Energy Procedia 16 (2012) 1526 – 1534, doi:10.1016/j.egypro.2012.01.239.
[3] Christian Wessels, Fabian Gebhardt and Friedrich W. Fuchs, "Dynamic Voltage Restorer to allow LVRT for a DFIG Wind Turbine", IEEE International Symposium on Industrial Electronics (ISIE), 2010, doi: 10.1109/ISIE.2010.5637336.
[4] J. Lopez, P. Sanchis, X. Roboam, L. Marroyo "Dynamic behavior of doubly fed induction generator during three phase voltage dips" IEEE Transactions on Energy Conversion, vol. 22, no. 3, 2007, pp. 709-717..
[5] M. Garcia-Gracia, M. P. Comech, J. Sallan, and A. Llombart, "Modelling wind farms for grid disturbance studies", Science direct, renewable energy, 33, 2008, pp. 2109-2121.
[6] M. Rahimi, M. Parniani, "Grid fault ride through analysis and control of wind turbines with doubly fed induction generators", Science direct, Electrical Power System Research, 80, 2010, pp. 184-195.
[7] S. Chondrogiannis, M. Barnes, "Specification of rotor side voltage source inverter of a doubly-fed induction generator for achieving ride-through capability", IET Renewable Power Generation, vol. 2, no. 3, 2008, pp. 139–150.
[8] Anca D. Hansen, Gabriele Michalke, "Fault ride-through capability of DFIG wind turbines" ScienceDirect, Renewable Energy 32 (2007) 1594–1610, doi:10.1016/j.renene.2006.10.008.
[9] Francois B., Yongdong Li, "Improved Crowbar Control Strategy of DFIG Based Wind Turbines for Grid Fault Ride-Through" Applied Power Electronics Conference and Exposition, 2009, pp. 1932 - 1938, doi. 10.1109/APEC.2009.4802937.
[10] Mingyu Wang, Bin Zhao, Hui Li, Chao Yang, Renjie Ye, Z. Chen, "Investigation of Transient Models and Performances for a Doubly Fed Wind Turbine under a Grid Fault" WSEAS TRANSACTIONS on CIRCUITS and SYSTEMS, Issue 11, Volume 10, November 2011.
[11] Omar Noureldeen, Mahmoud Rihan, BarakatHasanin, "Stability improvement of fixed speed induction generator wind farm using STATCOM during different fault locations and durations", ScienceDirect, Ain Shams Engineering Journal (2011) 2, 1–10, doi:10.1016/j.asej.2011.04.002.
[12] "MATLAB/Simulink Documentation". Available: http://www.mathworks.com.

